Journal of the Korean Physical Society, Vol. 66, No. 2, January 2015, pp. 301∼313

Evaluation of Breathing Patterns for Respiratory-gated Radiation Therapy Using the Respiration Regularity Index

Kwang-Ho Cheong, MeYeon Lee, Sei-Kwon Kang, Jai-Woong Yoon, SoAh Park, Taejin Hwang, Haeyoung Kim, KyoungJu Kim, Tae Jin Han and Hoonsik Bae*
Department of Radiation Oncology, Hallym University College of Medicine, Anyang 431-070, Korea

(Received 3 November 2014)

Despite the considerable importance of accurately estimating the respiration regularity of a patient in motion compensation treatment, not to mention the necessity of maintaining that regularity through the following sessions, an effective and simply applicable method by which those goals can be accomplished has rarely been reported. The authors herein propose a simple respiration regularity index based on parameters derived from a correspondingly simplified respiration model. In order to simplify a patient's breathing pattern while preserving the data's intrinsic properties, we defined a respiration model as a $\cos^4(\omega(t)\cdot t)$ wave form with a baseline drift. According to this respiration formula, breathing-pattern fluctuation could be explained using four factors: the sample standard deviation of respiration period (s_f), the sample standard deviation of amplitude (s_a) and the results of a simple regression of the baseline drift (slope as β, and standard deviation of residuals as σ_r) of a respiration signal. The overall irregularity (δ) was defined as $||\vec{\omega}||$, where $\vec{\omega}$ is a variable newly-derived by using principal component analysis (PCA) for the four fluctuation parameters and has two principal components (ω_1, ω_2). The proposed respiration regularity index was defined as $\rho = \ln(1 + (1/\delta))/2$, a higher ρ indicating a more regular breathing pattern. We investigated its clinical relevance by comparing it with other known parameters. Subsequently, we applied it to 110 respiration signals acquired from five liver and five lung cancer patients by using real-time position management (RPM; Varian Medical Systems, Palo Alto, CA). Correlations between the regularity of the first session and the remaining fractions were investigated using Pearson's correlation coefficient. Additionally, the respiration regularity was compared between the liver and lung cancer patient groups. The respiration regularity was determined based on ρ; patients with $\rho < 0.3$ showed worse regularity than the others whereas $\rho > 0.7$ was suitable for respiratory-gated radiation therapy (RGRT). Fluctuations in the breathing cycle and the amplitude were especially determinative of ρ. If the respiration regularity of a patient's first session was known, it could be estimated through subsequent sessions. Notably, the breathing patterns of the lung cancer patients were more irregular than those of the liver cancer patients. Respiration regularity could be objectively determined by using a composite index, ρ. Such a single-index testing of respiration regularity can facilitate determination of RGRT availability in clinical settings, especially for free-breathing cases.

PACS numbers: 87.19.St, 87.52.-g, 87.53.Vb, 87.56.-v
Keywords: Breathing pattern, Respiration regularity index, RPM system, Lung, Liver
DOI: 10.3938/jkps.66.301

I. INTRODUCTION

In radiation therapy, delivery of an appropriate dose to targets in the lung or the upper-abdominal regions is complicated by respiratory motion [1,2]. In one inhale-exhale cycle for example, a lung tumor can move as much as 30 mm [2]. Imaging and beam-delivery techniques have been developed to minimize the effects of organ motion, among which modalities, respiratory-gated radiation therapy (RGRT) and motion tracking techniques have become popular in the radiation oncology field [3–5]. In RGRT, the beam is on only during a pre-determined gating window interval. In the case of motion tracking techniques, multi-leaf collimator (MLC) leaves follow the target's motion while the beam is on and radiation is delivered. The newly-developed Vero tracking system is also appropriate for motion tracking [6], and a motion compensation technique is applied in CyberKnife, as well. Recent studies on the Synchrony of CyberKnife showed the possibility of margin reduction without sacrificing target coverage [7,8]. Moreover, Ernst introduced motion prediction and compensation methods to tackle in detail the problem of latency for

*E-mail: b8510@hallym.or.kr; Fax : +82-31-380-3913

quasi-periodic motion in robotic radiosurgery [9]. Although compensation for the target's motion is roughly possible by using several known algorithms, prediction still relies on breathing regularity.

Most breathing motion control techniques are based on the assumption that during a treatment session, not only does the breathing pattern not change [1,2] but the initial breathing pattern in the remaining fractions is maintained. However, if a patient's breathing is irregular, a dosimetric error more serious than that in conventional treatment can be incurred. This is an especially critical issue in stereotactic body radiation therapy (SBRT), in that the treatment time is longer than it is in conventional therapy and very high precision is required [10, 11]. Thus, the respiration regularity of a patient as well as the probability of maintaining that regularity through the following sessions must be estimated. However, this issue has not yet received adequate attention, despite the important information that is provided for treatment of patients with tumor motion. Most studies reported since the early 2000s, rather, have focused on overcoming the transient changes in irregular breathing patterns [12].

In this study, we investigated the factors that can determine the regularity of respiration, and then formulated a respiration regularity index based on parameters derived from a simplified respiration model. We then evaluated the respiration regularity and validity of the index by application to clinical cases. We determined that the initial regularity was maintained to the end of treatment by confirming the correlation between the regularity of the first session and the remaining fractions.

II. MATERIALS AND METHODS

1. Patient Selection and Acquisition of Respiration Signals

We randomly selected the respiration signals of liver cancer (Nos. 1 $\sim$ 5) and lung cancer patients (Nos. 6 $\sim$ 10) that had been treated in our facility from 2007 to 2010 (Table 1). We separated the lung cancer patients from the liver cancer patients owing to the possibility that the former had inferior respiration regularity relative to that of the latter [13]. Respiration signals were obtained using a real-time position management (RPM; Varian Medical Systems, Palo Alto, USA) system [14]. Although respiration signals can be acquired during either four-dimensional computerized tomography (4DCT) scanning or RGRT, we used only signals from treatment sessions because the 4DCT scanning time recorded in the exported RPM data was not long enough. The patients breathed freely, without any visual or audio guidance. A total of 11 respiration signals were extracted per patient (initial session: 1 signal, early session: 4 signals, middle session: 3 signals, final session: 3 signals); we set the first session as the reference for predicting the regularity variation thereafter. The patient information, including planning target volume PTV, tumor length in the cranial-caudal (CC) direction, uncontrolled and controlled tumor motion in CC direction, and RGRT gating window size, is displayed. The parameters were similar, except that the PTV volume of the liver cancer patients was more than twice that of the lung cancer patients.

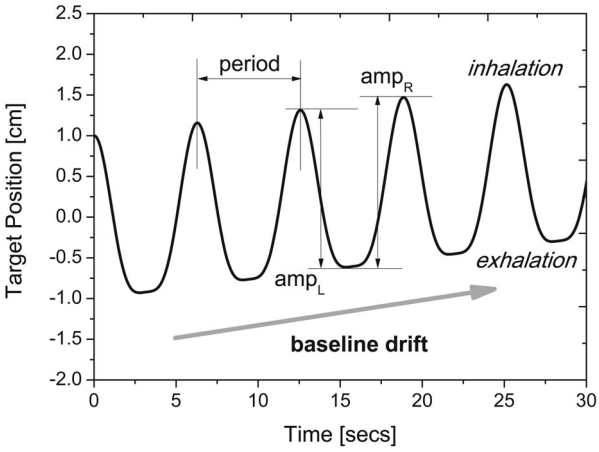

Fig. 1. Simplified breathing model using Eq. 1. The breathing pattern can be represented using a cosine^4 wave form with fluctuations in the respiration frequency, amplitude, and baseline.

2. Respiration-pattern Modeling

Clinically, multiple physiological factors, such as breathing period, lung volume change, inhalation time and exhalation time, and their ratio (exhalation-inhalation time ratio: EI ratio), are used to explain the breathing pattern. However, with respect to RGRT, tumor motion and baseline stability are additional critical factors that demand consideration. A respiration pattern is time-series data represented as a periodic function (*i.e.*, in a sine or a cosine wave form), though an actual breathing signal is more irregular and, thus, more difficult to standardize. A quasi-periodic function accounting for variations observed in real respiration is useful for a relatively precise simulation of human respiration motion [9], though sometimes a more simplified respiration form is sufficient for model-based analysis. In order to simplify a patient's breathing pattern while preserving the data's intrinsic properties, we defined the respiration formula as

$$Y(t) = A(t)\cos^4(\varphi(t)\cdot t) + B(t), \quad (1)$$

where A, φ, and B indicate the amplitude, period and baseline drift, respectively. Because each factor is a function of time, the regularity is considered to be adequate if each parameter's fluctuation is moderate. At the initial stage of this study, we investigated the correlations

Table 1. Patient information used in this study: PTV, tumor length in the cranial-caudal (CC) direction, uncontrolled and controlled tumor motion in the CC direction, and RGRT gating window size.

Study No.	Diagnosis	PTV volume (cm^3)	Tumor length (cm)	Tumor motion (cm)	Controlled tumor motion (cm)	Gating window (%)
1	Liver	651.6	9.1	0.9	0.3	38 – 62
2	Liver	2134.8	20.4	1.2	0.5	30 – 70
3	Liver	1004.8	15.6	1.3	0.4	38 – 63
4	Liver	748.5	11.1	1	0.3	40 – 70
5	Liver	189.4	8.1	1.1	0.5	30 – 70
		945.8 ± 727.1	12.86 ± 5.1	1.10 ± 0.15	0.40 ± 0.10	
6	Lung (L)	85.2	6.3	1.1	0.4	35 – 70
7	Lung (L)	597.2	17.8	1.4	0.5	30 – 70
8	Lung (R)	191.8	13.1	1	0.4	35 – 75
9	Lung (L)	1007.5	16.7	1.2	0.4	38 – 63
10	Lung (R)	284.2	10.4	0.6	0.2	40 – 60
		433.2 ± 373.6	12.86 ± 4.7	1.06 ± 0.30	0.38 ± 0.11	

among the variations in the period frequency, inhalation time, exhalation time, EI ratio, amplitude, and marker positions at the end of exhalation and at the end of inhalation, then, we defined, by using a principal component analysis (PCA), the major factors affecting respiration. From the preliminary result, we found that (1) strong correlations existed among the period, inhalation time, exhalation time and EI ratio; (2) strong correlations existed among the amplitude and marker positions at the ends of exhalation and inhalation; (3) explaining the respiration pattern by using variations in the period frequency and the amplitude is reasonable. Additionally, baseline changes in the sum had to be considered. Therefore, the respiration model in Eq. 1 is feasible. Ruan *et al.* followed a similar decomposition approach, including additional noise, in their work [15]; they did not focus on respiratory regularity. Fig. 1 provides a simple illustration of the model. Next, we will define the fluctuation parameters for each component in detail.

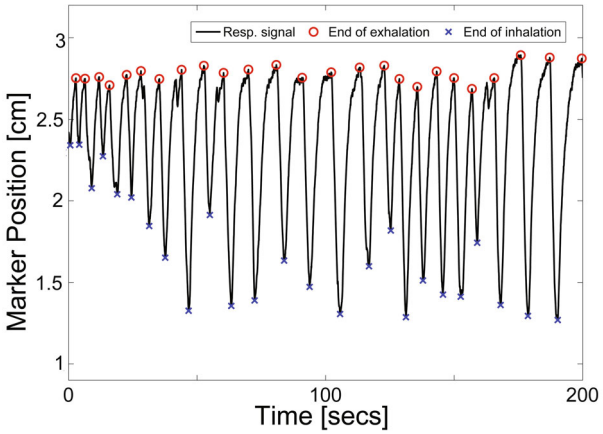

Fig. 2. (Color online) RPM system's 200-second respiration signal for a lung cancer patient (No. 10). The peaks at the end of exhalation (EE: o marks) and of inhalation (EI: x marks) are displayed.

A. Regularity of respiration cycle

Figure 2 is an actual lung cancer patient (No. 10)'s respiration signal acquired using the RPM system and used in this study. The amplitude, breathing frequency and baseline are unstable. Full exhalation is represented by the upper peaks, and full inhalation by their opposites. Hereafter, upper peaks represent the end of exhalation (EE) in all figures unless otherwise indicated. The frequency of the time-series data is commonly analyzed on the basis of the frequency domain spectra [16]; however, due to the wide distribution of periods, the characteristics of the respiration period are not clearly seen. Therefore, we defined "peak-to-peak", one EE to the next EE, as one respiration period; thus, correctly detecting peaks in a noisy signal is important. To determine whether each peak is significantly larger or smaller than the data around it, we used a peak detection algorithm that finds, according to a predefined threshold, local peaks and valleys in a noisy respiration signal. The distribution of respiration periods can then be modeled as a Gaussian distribution [17]; in this way, the characteristics of the period can be represented as sample mean and sample standard deviation. We confirmed the normality of this distribution by using a Q-Q plot. If there is no variation, the sample mean is the same as the nominal period but if the respiration cycle is not regu-

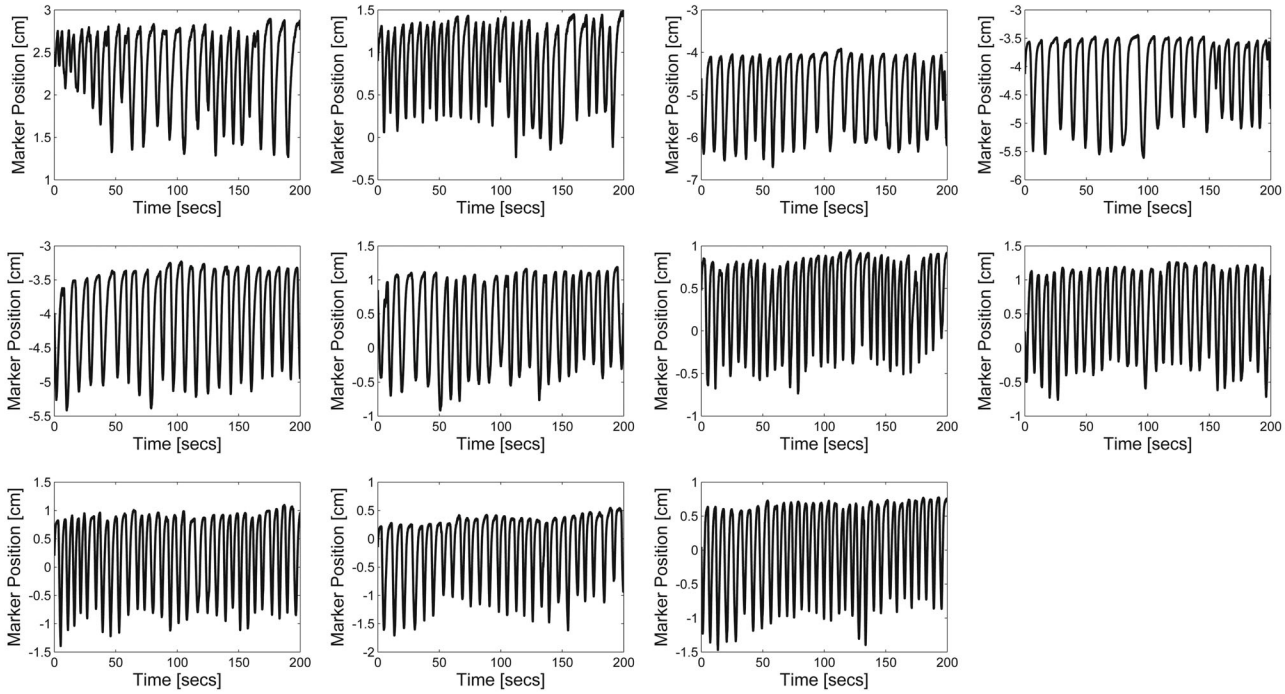

Fig. 3. RPM system's 11 respiration signals for a lung cancer patient (No. 10). The signals were from the 1 initial, 4 early, 3 middle, and 3 final sessions.

lar, the sample standard deviation will be increased. In other words, the sample standard deviation is the proper factor for explaining fluctuations in the respiration period. We defined the sample standard deviation of the respiration period as sf. The marker positions at the end of inhalation (EI) and at the EE, calculated automatically using in-house analysis tools with MATLAB 2011b (MathWorks Inc., Natick, USA), are also displayed in Fig. 2. SPSS 21 (IBM SPSS Inc., Armonk, USA) was used for further statistical analysis.

B. Regularity of amplitude

The amplitude of the respiration pattern at the i-th period was calculated using Eq. 2, where x is a marker position at the EE:

$$A_i = \frac{1}{2}(|x_{EE,i} - x_{EI,i}| + |x_{EI,i} - x_{EE,i+1}|), \qquad (2)$$

he amplitude is the average of the left- (amp_L) and right-side (amp_R) values for any inhalation peaks, as indicated in Fig. 1. Points that could not be located on a complete cycle were removed from the calculation. Figure 3 shows all of the 11 respiration signals for a lung cancer patient (No. 10). As indicated, the range of the amplitude varied among sessions due to marker-position and camera-angle variations. However, the overall magnitude of the amplitude generally did not change due to the fact that the magnitudes are absolute values normalized to the known intervals between two reflectors on a marker block. The distribution of amplitude ranges can be explained by using sample means and sample standard deviations of the breathing-cycle frequency [18]. We take the sample standard deviation of the amplitude (s_a) as the amplitude irregularity parameter.

C. Evaluation of baseline changes

Baseline changes can be considered, separately, according to either of two components: random changes and long-term drift [9]. Baseline long-term drift, also known as "baseline drift", is a common phenomenon in breathing patterns [19]. Generally, the baseline is defined as the position at the EE because it is more stable than it is at the EI [20]. In this study, we considered the baseline drift for positional variance only at the EE. The bases of the peaks varied with a simple increasing/decreasing trend or an oscillating trend. The simple increasing trend is clearly evident in Fig. 4. Although Lu *et al.* claimed that the baseline drift was not sufficiently large to affect the position of a tumor [11], it might, as the data indicate, become larger as time elapses over a very long session and the trend is sustained to the end of treatment. However, for a very long monitoring time, an oscillating pattern is more common. In those cases, it is more realistic to model the pattern as a cubic spline through the cycles [9]; however, we aimed to extract a

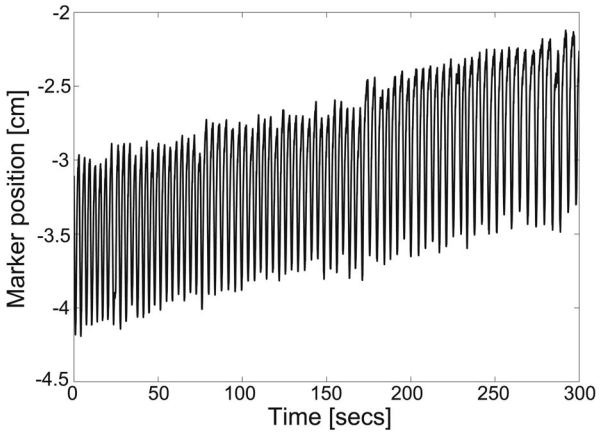

Fig. 4. Respiration signals for a liver cancer patient (No. 5) for a mid-term session. The baseline drift in the signal is obvious.

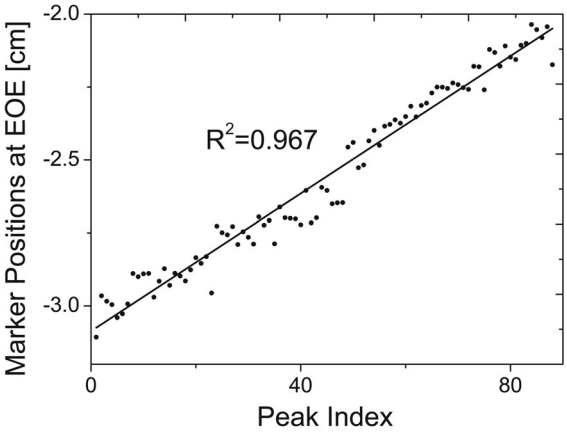

Fig. 5. Straight line estimated by using a simple regression as displayed on the scatter plot of the marker positions (·) at EE of the RPM signals shown in Fig. 4.

single parameter that could simply explain the baseline drift. Baseline drift, even if nonlinear, can be represented using the simple regression formula

$$\hat{Y} = \alpha_0 + \beta X + \epsilon, \tag{3}$$

where β and α_0 represent the slope and the intercept of a straight line, respectively, and ϵ is an error term (residuals), assuming that $\epsilon \sim \mathrm{N}(0, \sigma_r^2)$. We defined the standard deviation of residuals as σ_r, which accounts for random changes of the baseline. Thus, β and σ_r were used to quantitatively analyze the baseline changes in this study. Figure 5 shows the scatter plot and the straight line for a liver cancer patient (No. 5), where $\beta = 0.012$, $\alpha_0 = -3.076$, and the adjusted $R^2 = 0.967$.

3. Formulation of the Respiration Regularity Index

Even though four breathing-pattern fluctuation parameters (s_f, s_a, σ_r and β) are determined for a signal, using a single value incorporating all of them when determining respiration regularity is more convenient. However, given that these coefficients are possibly correlated, a simple combination might overestimate the breathing irregularity. A parameter-correlation matrix is provided in Table 2. As is obvious, strong correlations existed among the parameters, which fact called for consideration of the covariance of each correlation. We, therefore, implemented PCA and derived a new variable, $\overrightarrow{\omega}$. Generally, $\overrightarrow{\omega}$, as defined in Eq. 4, has fewer standardized principal components than the parameters do (in this case: 4):

$$\omega_i = l_{1,i} s_f + l_{2,i} s_a + l_{3,i} \sigma_r + l_{4,i} \beta, \tag{4}$$

where $l_{n,i}$ is a principal component coefficient, which is the factor loading divided by the square root of the i-th eigenvalue, $\sqrt{\lambda_i}$. The number of principal components can explain more than 80% of the variations of the overall respiration irregularity while satisfying $\lambda_i > 0.7$. We applied rotation using varimax for clear observation of the four fluctuation parameters. The overall irregularity of a patient's respiration can be explained using the Euclidean norm of $\overrightarrow{\omega}$, expressed in Eq. 5 and defined as δ:

$$\delta = ||\overrightarrow{\omega}|| \qquad (0 \le \delta < \infty). \tag{5}$$

Because our goal was to explain breathing-pattern regularity with a single number, we formulated a respiration regularity index (ρ) that could account for a patient's respiration regularity using δ. Respiration regularity can be regarded simply as $1/\delta$; however, as this is very sensitive to the variation of δ, we defined ρ as in Eq. 6 in order to narrow the otherwise impractically wide range of ρ:

$$\rho = \ln(1 + (1/\delta))/2 = \ln(1+\kappa)/2 \quad (0 < \rho < \infty), \tag{6}$$

where $\kappa = 1/\delta$. This is the final form of our proposed respiration index. Although the interval of ρ is $(0, \infty)$, it rarely diverges to ∞ unless $\delta = 0$; as such, it is not realistic for actual patient data. Even in the case where δ is 10^{-6}, for example an extreme case, ρ is merely 6.91.

Table 2. Parameter-correlation matrix of the fluctuating parameters s_f, s_a, σ_r, β.

	s_f	s_a	σ_r	β
s_f	1.000	0.771**	0.255**	−0.124**
s_a		1.000	0.520**	−0.328**
σ_r			1.000	−0.286**
β				1.000

** The correlation is significant at the 0.01 level (2-tailed).

4. Clinical Relevance of δ and ρ

A. Correlation between δ, ρ and tumor motion

Given the importance of confirming the clinical relevance of δ and ρ, we investigated the correlation between δ, ρ, the estimated controlled tumor motion range ($\theta_{T,1}$) and the over-travel range over a preset margin (upper and lower bounds) in the superior and the inferior directions (ξ_U and ξ_L) only within the RGRT gating period because we focused only on how target motion control was maintained during RGRT. Because we were already aware of the uncontrolled tumor motion range ($\theta_{T,0}$) and the gating window size (Δ), extracting signals inside the gating window by using the phase information recorded in the RPM data file. Each signal was cut off and then rescaled for overlapping. We assumed that the external marker signal was perfectly correlated with the internal target motion. Figures 6 and 7 show (a) respiration signals, (b) superposed respiration cycles, and (c) cropped signals based on . The respective normalized histograms for the patients' cropped respiration signals are displayed in Fig. 6(d) and 7(d). Figure 6 is an example of a relatively regular case while Fig. 7 shows an instance of irregular breathing and, consequently, of failure to track regularly through each cycle. Inside the gating interval, the lower bound (BL) is the same as the baseline, and the upper bound (B_U) is $B_L + \theta^*_{T,1}$, where $\theta^*_{T,1}$ is the nominal controlled tumor motion, that is, the internal target volume (ITV) margin for treatment. B_L was determined based on the median value of signals at the 50% phases and maximum travel ranges of the tumor for both cycles, and the cropped gated regions were determined to encompass signals in the 95% confidence interval (CI).

B. Correlation between δ, ρ and dosimetric error due to irregular breathing

We also investigated the correlation between δ, ρ and the dosimetric error due to irregular breathing pattern, considering only the phase-based gated RT. First, we needed to make a few assumptions for a RGRT dose simulation: (1) The external marker signal is perfectly correlated with the internal target motion; (2) the target is modeled simply as an elliptical shape, and we already know the length and motion range; (3) the target is conformal and fully covered by the prescribed isodose line; (4) radiation is delivered from beams arranged on the coplanar plane, and they contribute to the total dose evenly (thus, we can simplify the situation further: one beam is irradiated perpendicular to the target motion, as shown in Fig. 8); (5) no setup margin is considered; thus, the PTV is the same as the ITV, and each beam is exactly irradiated into the ITV volume; (6) each beam is delivered during the entire time recorded in the RPM data file. If there are no variations in respiration, the controlled tumor motion range will be within the preset

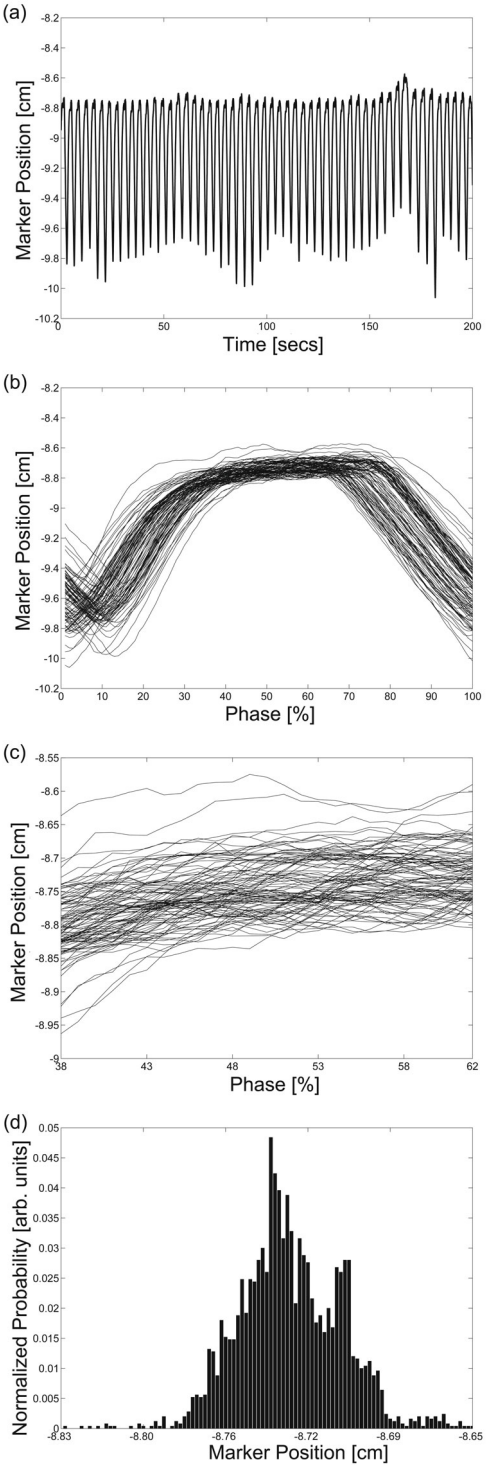

Fig. 6. Example of a regular breathing pattern (patient No. 1, session 1): (a) respiration signals, (b) superposed respiration cycles based on phase information in the RPM data file, (c) cropped signals within the RGRT gating window and (d) normalized histogram for the cropped respiration signal.

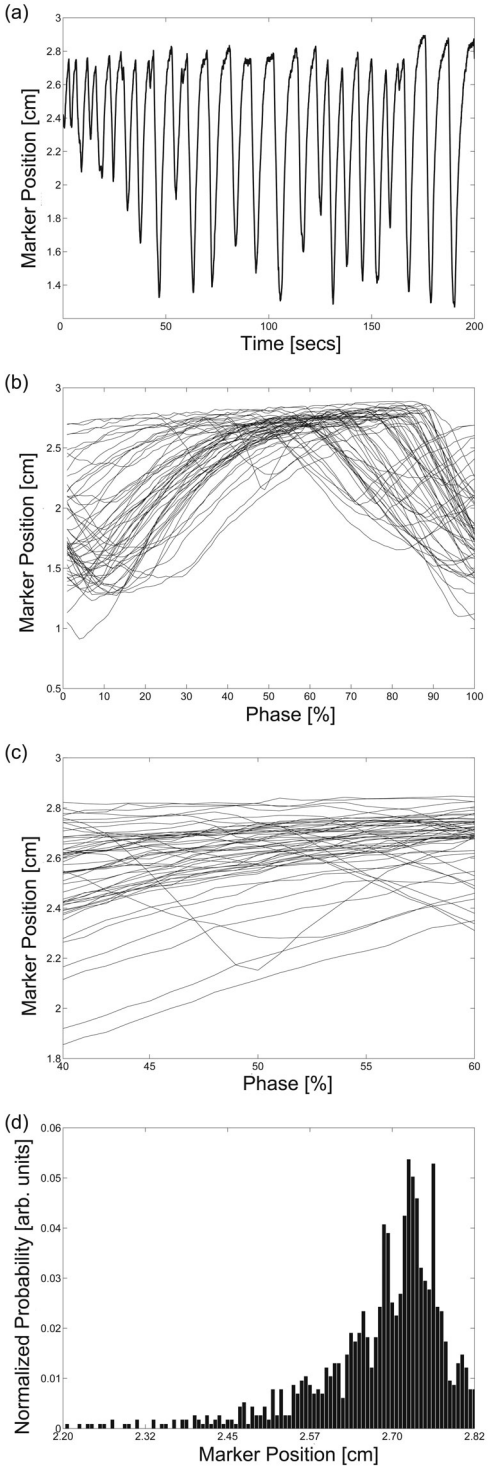

Fig. 7. Example of an irregular breathing pattern (patient No. 4, session 6): (a) respiration signals, (b) superposed respiration cycles based on phase information in the RPM data file, (c) cropped signals within the RGRT gating window and (d) normalized histogram for the cropped respiration signal.

interval, which is usually less than 0.5 cm; however, if variations increase during marker tracking, the system

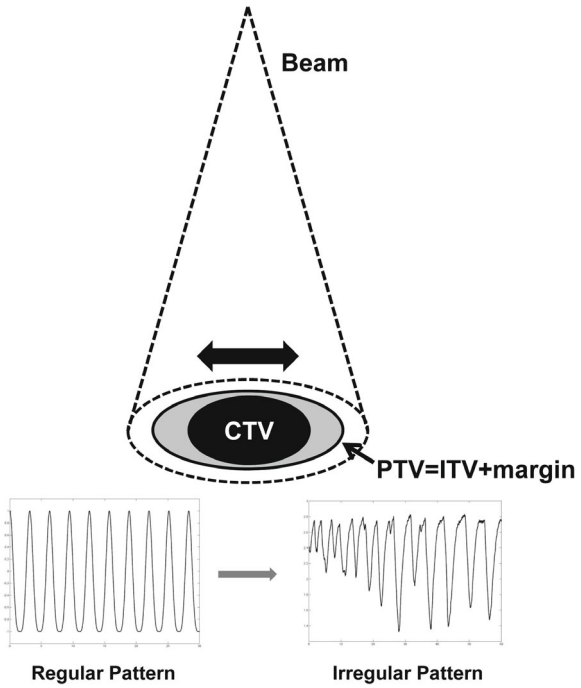

Fig. 8. Diagram of the beam irradiation to the target for the dose simulation. One beam is irradiated in a direction perpendicular to the target's motion.

might fail to deliver the correct dose to the target. Dosimetric error in terms of the missing volume, , is defined as

$$\varepsilon = (V_{PTV} - V_{pres})/V_{PTV}, \tag{7}$$

where V_{PTV} and V_{pres} stand for the total PTV volume and the PTV volume covered by the prescribed isodose line.

C. Comparison with Root-mean-Square (RMS) of Prediction Algorithms

To test the reliability of the proposed index, we compared the result with the relative RMS value from the Graphical Prediction Toolkit [21] using the MULIN [22] and SVRpred [23] algorithms. We employed the default setting in the toolkit. Relative RMS value (RMS_{rel}) is an index of the extent of improvement that can be achieved by using a prediction algorithm and is defined as the RMS value from predicted signals (RMS_{pred}) divided by the RMS value from non-predicted signals (RMS_{orig}) [9]. If RMS_{rel} is large, the evaluated respiration signal will be too irregular for feasible prediction. We compared δ, ρ, RMS and RMS_{rel} by utilizing the MULIN and the SVR_{pred} algorithms.

Table 3. Regularity indices (ρ) and fluctuation-explaining factors (s_f, s_a, σ_r, β, δ) of patients' breathing patterns (patients No.1 and 10). The indices and factors pertaining to the initial session are indicated in bold font.

Liver							Lung						
Pt #	s_f	s_a	σ_r	β	δ	ρ	Pt #	s_f	s_a	σ_r	β	δ	ρ
	0.345	**0.086**	**0.028**	**0.001**	**0.280**	**0.760**		**2.357**	**0.290**	**0.066**	**0.000**	**1.680**	**0.233**
	0.384	0.078	0.043	0.001	0.305	0.727		1.562	0.161	0.074	0.002	1.104	0.322
	0.334	0.098	0.025	0.001	0.280	0.760		1.854	0.300	0.079	0.000	1.376	0.273
	0.311	0.074	0.026	0.003	0.250	0.805		2.775	0.311	0.039	−0.001	1.947	0.207
	0.350	0.075	0.033	0.004	0.277	0.764		1.254	0.145	0.063	0.006	0.897	0.375
1	0.252	0.075	0.020	0.003	0.212	0.872	10	1.264	0.154	0.043	0.005	0.902	0.373
	0.527	0.105	0.047	0.001	0.412	0.616		0.837	0.115	0.056	0.002	0.615	0.483
	0.425	0.109	0.049	0.004	0.352	0.673		1.032	0.190	0.047	0.000	0.781	0.412
	0.216	0.073	0.033	0.002	0.194	0.910		0.972	0.147	0.051	0.004	0.718	0.436
	0.286	0.109	0.028	0.002	0.258	0.792		0.861	0.177	0.049	0.009	0.666	0.459
	0.328	0.096	0.028	0.004	0.275	0.767		0.872	0.168	0.036	0.004	0.663	0.460

5. Comparison of Respiration Regularity between Lung and Liver Cancer Patient Groups

For each patient and session, s_f, s_a, σ_r, β, δ and ρ were calculated to evaluate the regularity of each of the factors and the composite index. Then, we calculated the Pearson's correlation coefficient between the ρ of the reference session (ρ_0) and the mean ρ of the remaining sessions ($\overline{\rho^*}$) to determine any correlation between the two indices. A close correlation indicated a trend of respiration-pattern variation from the initial breathing pattern. We used an independent-samples t-test (Student's t-test) to determine whether differences in respiration regularity existed between the liver (G_{liver}) and the lung (G_{lung}) cancer patient groups. Only ρ was considered as a regularity factor, and a total of 55 cases per group were examined.

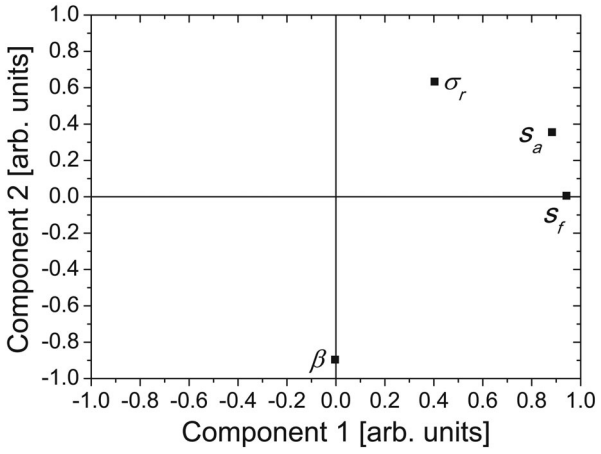

Fig. 9. Component plot in rotated space. β is less correlated with the others; therefore, a reverse relationship exists between $\{s_f, s_a, \sigma_r\}$ and β.

III. RESULTS

1. Respiration Regularity Index for Patients

From the PCA for the dataset used in this study, the estimated number of principal components was 2. This means that two principal components could explain 79% of the total variance. Each of the standardized principal components for $\overrightarrow{\omega} = (\omega_1, \omega_2)$ are included in Eq. 8:

$$\omega_1 = 0.63 s_f + 0.59 s_a + 0.27 \sigma_r,$$
$$\omega_2 = 0.36 s_a + 0.65 \sigma_r - 0.92 \beta, \quad (8)$$

where ω_1 is the positive combination of all parameters except β; the fluctuations in the period and the amplitude are dominant while all parameters except β are strongly correlated. Contrastingly, in ω_2, β is a dominant factor; ω_2 mainly considers the baseline drift. However, the contribution of ω_2 to δ is relatively small. Figure 9 shows a component plot in rotated space. As can be seen, β is less correlated with the others; correspondingly, a reverse relationship exists between them. Although the coefficients in Eq. 4 can be changed based on population data, δ did not vary significantly as we tested and obtained different $l_{n,i}$ for different datasets; therefore, Eq. 8 can be considered to be robust for routine clinical purposes of respiration-irregularity estimation. Fig. 10 shows the ρ (sorted in ascending order) for the patient data used in this study: $2 < \rho < 1.1$. It was stable, and accordingly, intuitively guessing a patient's respiration regularity was easy. Table 3 shows the s_f, s_a, σ_r, β, δ and ρ values for patients No. 1 and 10 and treatment session. The respiration regularity could be determined

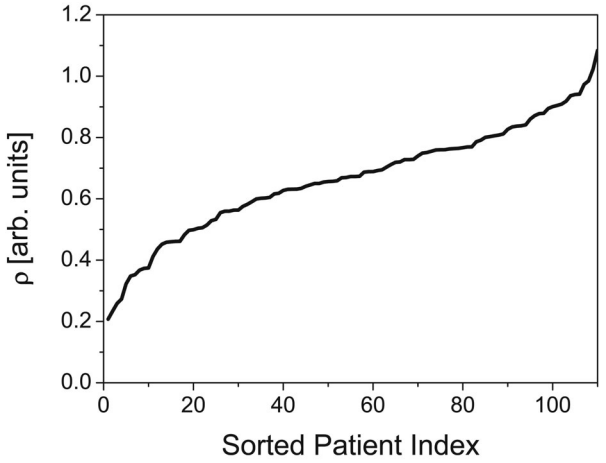

Fig. 10. Sorted ρ (in ascending order) for the patient data used in this study. The range of ρ is (0.2, 1.1).

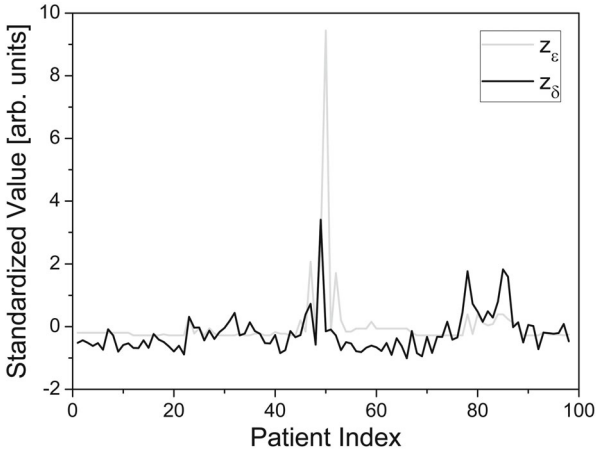

Fig. 11. Standardized distributions of the overall irregularity (δ) and the dosimetric error (ε). The two distributions show similar patterns.

Table 4. Correlation among δ, ρ, ε, the estimated controlled tumor motion range ($\theta_{T,1}$), and the over-travel range over preset margin in the superior and the inferior directions (ξ_U and ξ_L) only within the RGRT gating period.

	ρ	δ	ε	$\theta_{T,1}$	ξ_U	ξ_L
ρ	1.000	−0.898**	−0.214*	−0.216*	−0.594**	−0.285**
δ		1.000	0.262**	0.233*	0.623**	0.350**
ε			1.000	0.449**	0.622**	0.748
$\theta_{T,1}$				1.000	0.486**	0.604**
ξ_U					1.000	0.528**
ξ_L						1.000

* The correlation is significant at the 0.05 level (2-tailed).
** The correlation is significant at the 0.01 level (2-tailed).

based on ρ; fluctuations in the breathing cycle and the amplitude, moreover, were especially determinative of ρ [18].

2. Clinical Relevance of δ and ρ

Table 4 lists the correlations among β, δ, ε, $\theta_{T,1}$, ξ_U and ξ_L for the data on patients Nos. $1 \sim 9$. The last patient's data were not used for this analysis because $\theta_{T,0}$ and $\theta_{T,1}$ were relatively small compared those for to the other patients and would have skewed the trend for the entire population. A strong inverse correlation existed between δ and ρ, as is easily understood. Although the correlation between ρ and ε was not strong, the proposed index was correlated with the dosimetric error. This is clearer in the stronger correlation between δ and the other parameters. Standardized distributions of δ and ε are displayed in Fig. 11. Figure 12 shows the correlation between δ and ε in the form of simple regression data. Most of the values of the dosimetric error are located near y = 0 because the estimated error inside a gating interval was quite small. The estimated regression slope was very small as well, indicating that the probability of the PTV escaping the margin, correspondingly, were sufficiently small. However, when we considered the worst case, as represented by the values on the upper side of the graph, the probability increased. If we were to calculate the slope of a line passing through these large values, δ would be less than 2: in the present case, $\rho = 0.2$. However, we set $\rho = 0.3$ as the minimum condition for application of the RGRT safety margins. Moreover, $\rho > 0.7$ or $\delta < 0.35$ also would be regarded as suitable for RGRT. On the basis of the data in Table 4, we can say that if the breathing pattern is not good enough, the probability of the target's escape from the determined upper and lower bounds increases, and the missing target volume that cannot receive the proper dose increases.

3. Comparison with RMS of Prediction Algorithms

The correlations between δ and multiple RMS indices were not strong; however, a relatively strong correlation existed between RMS_{SVR}, $(\mathrm{RMS}_{SVR})_{Rel}$ and ρ or δ/ Figure 13 shows the standardized distributions of δ and $(\mathrm{RMS}_{SVR})_{Rel}$. Although the matching was not good, we can see a similar trend through the data, indicating that the proposed ρ and δ are useful and applicable to the evaluation of patients' respiration regularity.

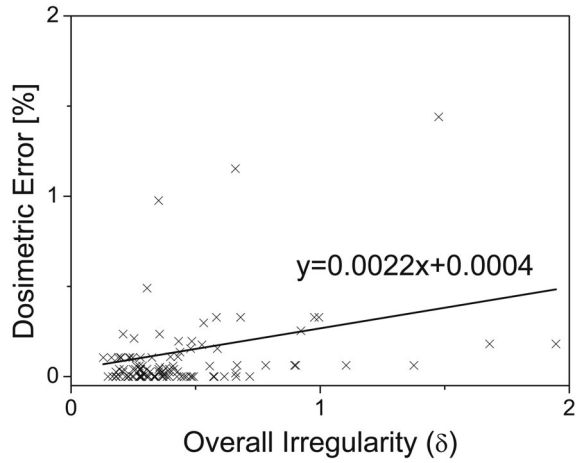

Fig. 12. Relationship between the overall irregularity (δ) and the dosimetric error (ε, x marks) as a simple regression.

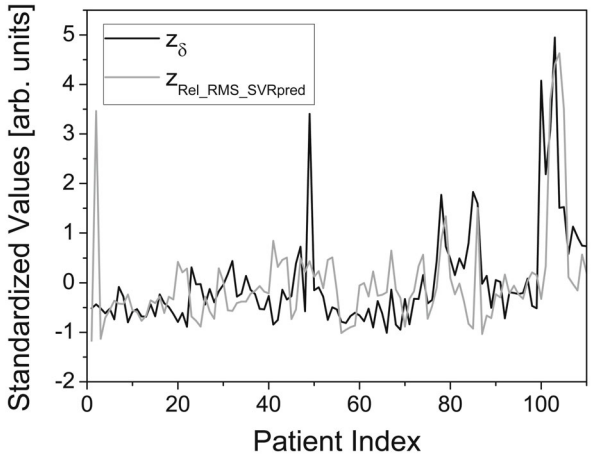

Fig. 13. Standardized distribution of the overall irregularity (δ) and the relative $(\mathrm{RMS}_{SVR})_{Rel}$. Although the matching is not good, we can see a similar trend through the data.

4. Prediction of Patients' Respiration Regularity

The ρ_0 and the $\overline{\rho^*}$ for each patient are listed in Table 5. The Pearson's correlation coefficient (R) for the two datasets was 0.951, $p < 0.01$, reflecting a very strong, positive correlation between them. This indicated that if the ρ_0 for a patient is known, the respiration regularity of that patient through subsequent sessions can be predicted. Patients with a high ρ_0 tended to sustain breathing regularity. Nonetheless, there were abnormal cases showing very irregular patterns even with ρ_0 of more than 1 [24]. Figure 6 plots examples of these cases (No. 5): the initial (Fig. 14(a)) and the mid-term (Fig. 14(b)) breathing and ρ are displayed ($\rho_0 = 0.669$ and $\rho_4 = 0.259$); however, the abnormally irregular patterns in Fig. 14(b) seemed to be due to coughing; thus, they were manually removed, and the estimation was repeated (Fig. 14(c)). In this case, $\rho_{4,mod}$ was increased to 0.476.

Table 5. Respiration regularity index (ρ) for the initial session (ρ_0), mean ($\overline{\rho^*}$), and standard deviation (s_{ρ^*}) of ρ for all sessions except the initial session

	ρ_0	$\overline{\rho^*}$	s_{ρ^*}
Patient 1	0.760	0.769	0.086
Patient 2	0.839	0.802	0.093
Patient 3	0.529	0.625	0.068
Patient 4	0.654	0.720	0.118
Patient 5	0.669	0.634	0.183
Patient 6	0.900	0.862	0.111
Patient 7	0.631	0.744	0.169
Patient 8	0.353	0.488	0.083
Patient 9	0.754	0.671	0.090
Patient 10	0.233	0.380	0.089

Table 6. Mean ($\overline{\rho}$), median ($\widetilde{\rho}$), and standard deviation (s_ρ) of ρ for the liver and the lung cancer patient groups

Group	No of signals	Mean ($\overline{\rho}$)	Median ($\widetilde{\rho}$)	SD (s_ρ)
Liver	55	0.708	0.719	0.130
Lung	55	0.624	0.631	0.211

5. Comparison of Respiration Regularity between Lung and Liver Cancer Patient Groups

Table 6 provides a basic statistical summary of the two patient groups. The sample mean and median ρ of G_{liver} were larger than those of G_{lung}. Fig. 15's boxplots of the two groups also show this obvious discrepancy. The median ρ ($\widetilde{\rho}$) for G_{liver} was 0.719, but for G_{lung}, it was 0.631. The interquartile range (IQR) for G_{liver} was narrower than that for G_{lung}; the IQR of G_{lung} was wider for the larger values, indicating that the breathing patterns of the lung cancer patients were more irregular than those of the liver cancer patients. In the independent-samples t-test results, a significant difference existed in the mean values ($p < 0.001$, 2-tailed); thus, we can say that the respiration regularity between the two groups was quite different. In fact, some patients, due to their severe breathing irregularity, would be deemed unsuitable for RGRT. Shirato *et al.* showed that tumor motions within the lungs and the liver differ according to the corresponding anatomical dissimilarities [13]. Lu *et al.*, however, reported no significant differences between the lung-cancer and the upper-abdomen-cancer patient groups [11].

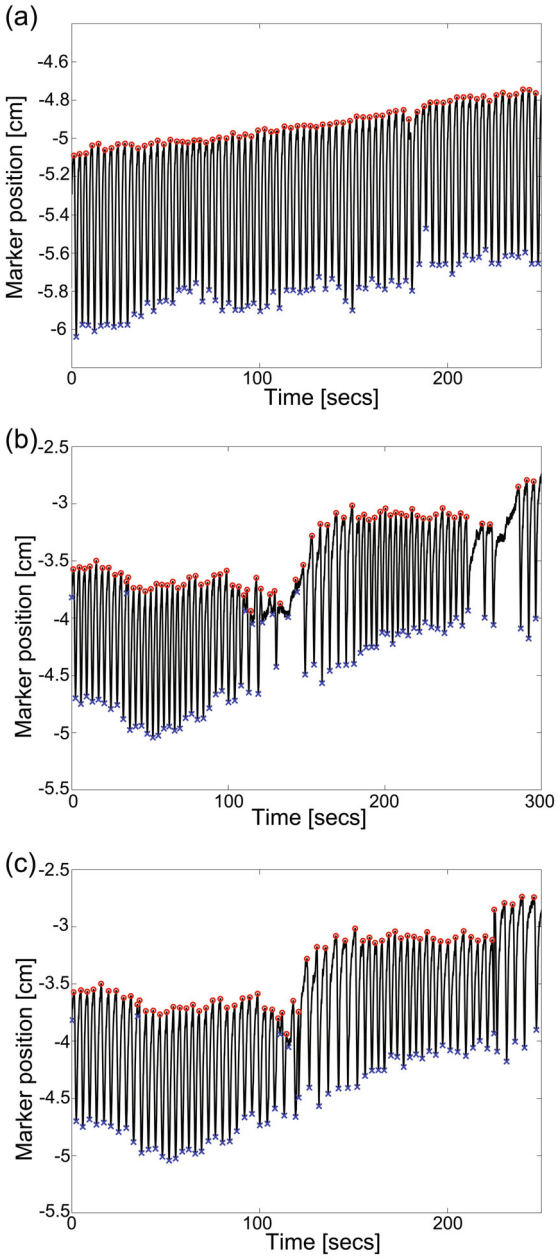

Fig. 14. (Color online) Respiration signals in (a) the initial and (b) the middle sessions of a liver cancer patient (No. 5), whose breathing pattern was estimated as regular in the initial session but became very irregular in the middle session. $\rho_0 = 0.669$, $\rho_4 = 0.259$. (c) Abnormally irregular pattern that was manually removed from the signal. $\rho_{4,mod} = 0.476$. The peaks at the end of exhalation (EE: o marks) and at the end of inhalation (EI: x marks) are also displayed.

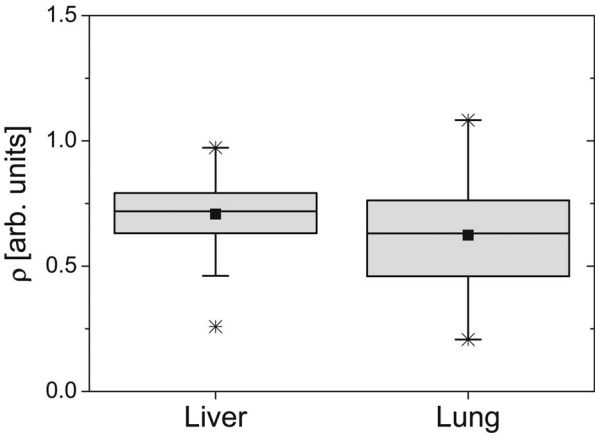

Fig. 15. Boxplots of the liver (G_{liver}) and the lung (G_{lung}) cancer patient groups showing obvious discrepancies. These results indicate that the respiration regularities of the two groups were quite different; specifically, the regularity of G_{liver} was better than that of G_{lung}.

IV. DISCUSSION

In this study, we defined a respiration regularity index (ρ) based on a breathing-pattern model. Fluctuations in the breathing cycle (s_f), amplitude (s_a), and baseline-drift residuals of the simple regression (σ_r) and the baseline-drift slope (β) were used to formulate the index. The fluctuation of each factor was distributed in a Gaussian form, and the range of the fluctuation could be explained using a sample standard deviation. The proposed index showed good validity as an explanatory tool for respiration regularity (indeed, the numerical information it provided will be applied to an upcoming respiration study). We did not employ the sample mean values of the respiration period or the amplitude in the evaluation because their differences are not critical factors in estimating the respiration regularity. For example, suppose that a patient has a breathing cycle of 3 seconds in the initial session, which is then lengthened to 5 seconds in the following session: RGRT can be said to be available for both cases, provided that the breathing cycle is maintained regularly during the session because RPM's respiration prediction utility is based only on the regularity of the signal of the given session. This, in fact, is shown in Figs. 6 and 7. Especially for severely, irregular breathing patterns, one respiration cycle cannot be accurately determined and will invoke target positional and dosimetric errors. This is why we focused on factor fluctuations in the present study. However, the dosimetric error was insignificant in all cases except the extremely irregular ones. This probably can be ascribed to the very small residual motion (on the order of a few millimeters) relative to the total target length. In Fig. 6(c), we can see that the cropped cycles are collected around the baseline. However, in Fig. 7(c), a more irregular pattern is shown. These trends were also clearly represented in each normalized histogram. The histogram indicates the probable means by which the target escapes the bounds. Obviously, the target in Fig. 7(d) can move over the upper bound even though the patient is undergoing RGRT. This is the reason we are interested in ξ_U

and ξ_L. One other issue concerns the baseline. Generally, baseline drift is ignored; therefore, no margins are applied to compensate for baseline changes, even when the drift is dominant inside a gating window, because the effects of amplitude and period fluctuations are relatively small. The interval of the baseline for the 95% CI will be a hint to the margins needed to compensate for baseline changes and prevent moving above B_L. On the other hands, β simply can be a predictor for baseline drift for less than 10 minute's monitoring.

Acquiring a respiration signal (sample) is a kind of sampling process that selects signals within a certain time period of a patient's overall breathing cycle (population); indeed, relative to an entire breathing cycle, an obtained respiration signal is very short. Although a breathing pattern is assumed to be repeated continuously, we cannot ascertain with complete certainty that the signal represents the patient's breathing pattern. Therefore, recording data sufficient to cover the entire treatment time is recommended. Moreover, the uncertainties of the fluctuation parameters also depend on the number of detected peaks at EI and EE. For example, when we calculate s_f, at least 30 EE positions are necessary, and the required recording time is a minimum of $30{\cdot}\overline{X_f}$, where $\overline{X_f}$ is a sample mean period of a respiration signal X. If $\overline{X_f} = 5$ seconds, > 150 seconds of recording is recommended. In the present study, we used around 300 seconds of data. The sampling time also affects the slope (β) of the line in a simple regression. Even though β, owing to its very small value, does not affect ρ much, σ_r strongly depends on it. Therefore, the respiration signal should be investigated before calculating ρ.

The respiration regularity index can be estimated after 4DCT acquisition or during RGRT. If the respiration signals obtained during 4DCT acquisition are used to estimate ρ, a recording time long enough to minimize the uncertainties is recommended. The respiration regularity index also can be used to estimate breathing patterns for other modalities such as fluoroscopy, spirometry, or Cyberknife. Generally, tumor-motion data are provided in a time-series format, which is suitable for evaluation of motion trends.

The proposed index, it should be noted, is sensitive to the peaks in the respiration signals. In the present analysis, whereas the exported RPM signals provided phase-angle-based peak and valley information, this could not be used because for patients with an irregular breathing cycle, the peaks were located at unexpected positions. Given the importance of finding the proper positions of the peaks at the EE and the EI, we employed our own peak detection algorithm.

Kissick *et al.* [17] analyzed longitudinal breathing motion in a simulation study. They used mean (μ) and δ terms (different terms from this study) to explain the distributions and the breathing-induced variations of the period, amplitude and baseline offset. They processed δ merely as a limiting factor in their simulations, specifically by assigning maximal values to each parameter. Wu *et al.* [25] reported tumor respiratory motion as determined in various statistical analyses; they used the concepts of state duration, cycle and state distance to model respiration signals. This approach, whereas it can yield useful information about the respiration pattern of a patient, does not provide intuitive parameters. In the present study, the actual respiration signal did not manifest itself in the $cos^4(\omega(t) \cdot t)$ wave form, but rather in a "saw tooth" pattern. The parameters that we needed, though, were calculated in the peak-to-peak manner, as detailed in Section II.2. Thus, the actual breathing pattern was not a critical issue: the parameters were almost the same, even when the actual signals were simplified in the sine wave form by using Eq. 1, and a patient's respiration pattern represented in that form using s_f, s_a, σ_r and β. Although we emphasized the respiration regularity index ρ, both ρ and δ can be useful single parameters for estimating the regularity or irregularity of breathing patterns.

Prediction of inter-fractional respiration regularity from a macroscopic point of view is also important to any determination of RGRT suitability. Notwithstanding, most prediction studies have emphasized intra-fractional forecasting, even when future breathing patterns could be predicted only a few seconds in advance [5,12,26,27].

The RMS index in Section II.5 as applied to the evaluation of the prediction ability is not intended for respiration regularity estimates; however, we compared ρ and δ with them simply because RMS values are correlated with the repeatability of a respiration signal's unit cycle. Whereas we attempted to investigate the clinical relevance of ρ and δ, the quantitative evidence remains relatively lacking; moreover, the $\rho > 0.3$ criterion for RGRT needs to be confirmed with larger populations in further studies. Nonetheless, despite the small number of patients reviewed in our statistical analysis, we were able to derive a regularity index from the data and properly apply it to clinical cases. Moreover, we were able to detect breathing-pattern transitions as the session proceeded by selecting a total of 11 sets from the initial, early, middle, and final sessions rather than randomly.

V. CONCLUSION

We were able to objectively determine the respiration regularity by using a composite index by which the breathing-cycle characteristics could be effectively explained. Additionally, we showed that by means of estimating ρ_0, a patient's future respiration regularity could be predicted. Single-index testing of respiration regularity can significantly facilitate determination of RGRT availability in clinical settings, especially for free-breathing cases.

ACKNOWLEDGMENTS

This work was supported by the Radiation Technology R&D program through the National Research Foundation of Korea funded by the Ministry of Science, ICT & Future Planning (No.2013043498).

REFERENCES

[1] K. M. Langen and D. T. Jones, Int. J. Radiat. Oncol. Biol. Phys. **50**, 265 (2001).
[2] P. J. Keall *et al.*, Med. Phys. **33**, 3874 (2006).
[3] A. Krauss, S. Nill and U. Oelfke, Phys. Med. Biol. **56**, 5303 (2011).
[4] D. Ruan, J. A. Fessler and J. M. Balter, Med. Phys. **35**, 782 (2008).
[5] G. C. Sharp, S. B. Jiang, S. Shimizu and H. Shirato, Phys. Med. Biol. **49**, 425 (2004).
[6] D. Verellen, T. Depuydt, T. Gevaert, N. Linthout, K. Tournel, M. Duchateau, T. Reynders, G. Storme, and M. De Ridder, Cancer Radiother. **14**, 446 (2010).
[7] M. Hoogeman, J. B. Prevost, J. Nuyttens, J. Poll, P. Levendag and B. Heijmen, Int. J. Radiat. Oncol. Biol. Phys. **74**, 297 (2009).
[8] E. W. Pepin, H. Wu, Y. Zhang and B. Lord, Med. Phys. **38**, 4036 (2011).
[9] F. Ernst, Compensating for Quasi-Periodic Motion in Robotic Radiosurgery, (Springer, New York, 2012).
[10] S. H. Benedict *et al.*, Med. Phys. **37**, 4078 (2010).
[11] W. Lu, P. J. Parikh, J. P. Hubenschmidt, J. D. Bradley and D. A. Low, Med. Phys. **33**, 2964 (2006).
[12] P. S. Verma, H. Wu, M. P. Langer, I. J. Das and G. Sandison, Comput. Sci. Engin. **13**, 24 (2011).
[13] H. Shirato, Y. Seppenwoolde, K. Kitamura, R. Onimura and S. Shimizu, Semin. Radiat. Oncol. **14**, 10 (2004).
[14] S. S. Vedam, P. J. Keall, V. R. Kini, H. Mostafavi, H. P. Shukla and R. Mohan, Phys. Med. Biol. **48**, 45 (2003).
[15] D. Ruan, J. A. Fessler, J. M. Balter and P. J. Keall, Phys. Med. Biol. **54**, 4777 (2009).
[16] F. Ernst, A. Schlaefer and A. Schweikard, Med. Phys. **38**, 5569 (2011).
[17] M. W. Kissick, X. Mo, K. C. McCall, L. K. Schubert, D. C. Westerly and T. R. Mackie, Phys. Med. Biol. **55**, 2983 (2010).
[18] Y. D. Mutaf, J. A. Antolak and D. H. Brinkmann, Med. Phys. **34**, 1615 (2007).
[19] S. Nishioka, T. Nishioka, M. Kawahara, S. Tanaka, T. Hiromura, K. Tomita and H. Shirato, Radiother. Oncol. **86**, 69 (2008).
[20] S. Vedam, L. Archambault, G. Starkschall, R. Mohan and S. Beddar, Med. Phys. **34**, 4247 (2007).
[21] http://www.Rob.Uni-Luebeck.De/Node/117#downloads.
[22] F. Ernst and A. Schweikard, Int. J. CARS. **3**, 85 (2008).
[23] F. Ernst and A. Schweikard, Int. J. Comput. Assist. Radiol. Surg. **4**, 439 (2009).
[24] D. Ruan, Phys. Med. Biol. **55**, 3885 (2010).
[25] H. Wu, G. C. Sharp, Q. Zhao, H. Shirato and S. B. Jiang, Phys. Med. Biol. **52**, 4761 (2007).
[26] S. S. Vedam, P. J. Keall, A. Docef, D. A. Todor, V. R. Kini and R. Mohan, Med. Phys. **31**, 2274 (2004).
[27] K. C. McCall and R. Jeraj, Phys. Med. Biol. **52**, 3455 (2007).